ASD TECHNICAL REPORT 61-686
PART I

INFLUENCE OF CARBON CONTENT AND SUBSTRUCTURE ON CLEAVAGE IN IRON SINGLE CRYSTALS

D.A. Hay
B.L. Averbach

Alloyd Electronics Corporation

April 1962

Directorate of Processes and Materials
Contract AF 33(616)-6454
Contract AF 33(616)-7091, Phase I
Project 7021

AERONAUTICAL SYSTEMS DIVISION
AIR FORCE SYSTEMS COMMAND
UNITED STATES AIR FORCE
WRIGHT-PATTERSON AIR FORCE BASE, OHIO

ASD ~~TECHNICAL REPORT~~ 61-686, pt 1
~~PART I~~

INFLUENCE OF CARBON CONTENT AND SUBSTRUCTURE ON CLEAVAGE IN IRON SINGLE CRYSTALS

D.A. Hay
B.L. Averbach

Alloyd Electronics Corporation

April 1962

Directorate of Processes and Materials
Contract AF 33(616)-6454
~~Contract~~ AF 33(616)-7091, ~~Phase I~~
Project 7021

AERONAUTICAL SYSTEMS DIVISION
AIR FORCE SYSTEMS COMMAND
UNITED STATES AIR FORCE
WRIGHT-PATTERSON AIR FORCE BASE, OHIO

ABSTRACT

The influence of substructure and carbon content on the ductile-brittle transition temperature were studied in iron single crystals. It was found that increases in carbon content (from 0.0005% to 0.030%) raised the transition temperature considerably. Small amounts of pre-straining at room temperature before sub-zero testing inhibited twin formation. In cases where twins were formed, many micro-cracks were found in twins and at twin boundaries in fractured crystals. In some cases, micro-cracks were also found in the matrix of fractured crystals.

This technical documentary report has been reviewed and is approved.

E. M. Kennedy Jr

E. M. KENNEDY, JR., LT. COL., USAF
Chief, Advanced Metallurgical
Studies Branch
Metals and Ceramics Laboratory
Directorate of Materials and Processes

TABLE OF CONTENTS

LIST OF TABLES

LIST OF FIGURES

I. INTRODUCTION

In recent years several theories have evolved on the probable role of dislocations and substructure in the cleavage fracture of iron and other body centered cubic materials. Many of these theories, such as the one suggested by Stroh[1], postulate a dislocation pile-up at a grain or twin boundary to initiate a cleavage crack. On the other hand, Cottrell[2] has suggested that cleavage cracks could be formed by the coalescence of two slip bands. Somewhat different amounts of preliminary slip are required in each of these theories.

According to the Stroh hypothesis, a microcrack once formed will not stop but will continue across the entire specimen. The Cottrell theory predicts the formation of stable microcracks and also indicates the maximum size of a stable microcrack. Microcracks have been found in specimens which had been loaded just below the fracture stress[3], but they were an order of magnitude larger than those predicted by Cottrell. On ther other hand recent observations[4] on other steels have failed to reveal microcracks. Therefore, it appears that neither the Stroh nor the Cottrell theoreis are completely satisfactory, and the role of substructure and composition are still obscure.

The Cottrell theory predicts stable microcracks of approximately one grain diameter. Thus the first cleavage crack should travel entirely across a single crystal, provided that it was not stopped by subboundaries or other obstructions. Therefore, the size of microcracks, in single crystal specimens, was investigated in order to further understand the mechanism of crack nucleation and propagation. However, it was observed here that twinning occurs prior to fracture in most single crystal specimens and it became evident that the twin formation may also provide a microcrack mechanism in single crystals.

In order to provide suitable conditions for cleavage rather than slip, it has been considered that the dislocations in the vicinity of the pile-up are pinned. It has been suggested that these dislocations are pinned by interstitial carbon atoms and that the avalanche of dislocations at the yield point provides the large number of dislocations required for crack formation. This investigation was undertaken to determine the role of dislocations in the formation of microcracks in single crystals of iron, and the interaction of interstitial carbon atoms with the dislocations. During the first part of this work single crystals of iron with carbon contents in the range 0.0005 - .03 weight percent were prepared. The methods for the measurement of dislocation density in iron crystals were also developed further. An x-ray rocking curve method had been used for aluminum and copper crystals and this was extended to iron. However, it was felt that an etch-pit method would be useful since it is relatively more rapid and can also provide some information on the dislocation arrays. Since etch pit methods are frequently unreliable, it was necessary to investigate promising etchants by means of the x-ray method. It appears that a quantitative etch for iron crystals has been found.

A part of this work involved the introduction of substructure by means of deformation and annealing treatments. It was necessary to calibrate the etching reagent in cases where fresh dislocations produced by deformation were present. This was especially needed since twinning in iron is inhibited by prior deformation and it was anticipated that this would influence the fracture behavior.

The single crystals were tested in tension at various sub-zero temperature. After tensile testing, the crystals were examined metallographically for twins and microcracks. Observations on the role of substructure and carbon content on the cleavage behavior of these iron crystals are summarized in the following sections.

II. EXPERIMENTAL METHODS

A. Preparation of Single Crystals

Large single crystals or iron containing varying amounts of carbon were grown by a gradient anneal method. Specimens from various heats of vacuum melted iron were heat treated to achieve an initial grain size of ASTM 5-7. The specimens were then strained approximately 2% by passing a Luder's band through the specimen. They were then machined to the configuration shown in Figure 1. The specimens were then slowly drawn through a furnace having a steep temperature gradient, slotted end first, in a dry hydrogen atmosphere at a peak temperature of 1600°F. The traveling speed of the furnace was approximately 1 cm/hr.

B. X-Ray Determination of Substructure

The orientation of the crystals was determined by a Laue back reflection technique. The surface preparation consisted of an electropolish to remove surface irregularities and a nital etch. Rocking curves were then run for these crystals on an x-ray double crystal recording spectrometer used in the parallel position. The specimen served as the first crystal and was rocked through the (200) diffraction peak. The second crystal was an iron crystal chosen because of its cube face orientation and a high degree of perfection compared to the other samples tested. The primary beam was defined by two sets of slits so that the area of the sample irradiated was 4 mm. square. The diffracted primary beam was defined by a set of vertical slits to reduce vertical divergence. These slits selected a beam .005 in. high to impinge on the analyzing crystal. The total vertical divergence was approximately 1/2 minute. The diffracted beam from the analyzing crystal was monitored by a Geiger counter whose output was measured by a scaler and counting rate meter.

The rocking curves for these specimens were measured using two x-ray wavelengths, Cu Kα and Cr Kα. Although copper Kα will fluoresce iron, this was not a problem since it was still possible to achieve a good peak to background ratio.

The results of these measurements were then analyzed according to the method of Hordon and Averbach[5]. It has been shown that the shape and breadth of an x-ray diffraction peak taken from a parallel position double crystal spectrometer is independent of wavelength distribution and slit width. By reducing the vertical divergence, the instrumental broadening may be reduced to a minimum and the rocking curve width may be related to the spatial arrangements of defects such as edge and screw dislocations. The presence of dislocations in a crystal will result in local lattice tilting, in local strains, in the presence of subboundaries and in a possible bending of the lattice planes. A given distribution of dislocations may result in several of these effects and the analysis must indicate consistent dislocation densities arising from the individual diffraction effects. Assuming the rocking curves to be Gaussian in shape and assuming Gaussian distribution of rocking curve components due to lattice tilting α, lattice strain ϵ, particle size L and uniform lattice bending r, the measured half-breadth β_m (width at one-half peak intensity) is given by:

$$\beta_m = \beta_o{}^2(1) + \beta_o{}^2(2) + \beta_\alpha{}^2 + \beta_\epsilon{}^2 + \beta_L{}^2 + \beta_r{}^2 \qquad (1)$$

where β_o (1) and β_o (2) are the natural half-breadths for the specimen and the analyzing crystals, and β_α, β_ϵ, β_L and β_r are the line breadths due to lattice tilting, lattice strain, particle size and uniform lattice bending respectively.

The values of β_o may be calculated from the equation given by Darwin[6], and the broadening associated with particle size and lattice bending may be neglected for crystals subjected to small tensile strains[5]. There are thus two unknowns and observations of half width using two x-ray wavelengths is sufficient to determine the broadening associated with lattice tilting and local strains. Since these effects are derived from the same set of dislocations, the dislocation density calculated from either broadening should be identical. In practice, the two values agreed reasonably well.

C. Determination of Dislocation Density by Etch Pit Techniques

Dislocation etch-pit methods have been developed for iron. In order for these etch-pits to be seen it is necessary for carbon or other interstitial atoms to be present. Several etchants were tried since some reagents appeared to be more useful for some crystallographic orientations. Etch pits were counted and compared with the dislocation densities obtained from x-ray rocking curves on the same specimens.

The etching reagents and the results are listed below:

2% Nital - Very good for samples oriented to (100) plane. Does not bring out definitive etch pits on other orientations. A suitable etching time for (100) plane is 15 sec.

2% Nital - Containing 2% saturated Picral - Results similar to plain Nital.

Saturated Picral - In order to see the etch pits, heating is necessary after etching.

Frye's Reagent - Very good for all orientations but the etching time was dependent on the orientation. The etching time ranged from 15 sec. to 1.5 min.

A reproducible method of counting the etch-pits was evolved. It was found that more accurate counts could be made while observing the surface on a metallograph than could be made from a photomicrograph. Therefore, a filar eyepiece was used at a total magnification of 450X. Several traverses were made on each specimen, counting the pits that intersected a line of known length. The average of these readings was then used to calculate the density of pits per square centimeter.

D. Low Temperature Tensile Testing

The single crystals were tested in tension at various sub-zero temperatures using a Houndsfield tensometer which has been equipped with a low temperature tension chamber. Stress-strain curves were recorded and pertinent facts relating to the type of fracture were noted. Some specimens were also prestrained at room temperature and annealed in some cases prior to testing at low temperatures in order to investigate the influence of substructure.

III. RESULTS

A. X-Ray Diffraction

The double crystal x-ray rocking curves indicated inhomogeneities along the length of the specimens.

Both the half-breadths and the intensities of the rocking curves differed from point to point along the crystals. Table I lists the half-breadths of crystals obtained with Cu Kα and Cr Kα radiations in the as grown condition and in a few cases after straining at room temperature.

Each of the half-breadths noted is the average of at least four measurements. Attempts were made to irradiate the same areas with both radiations but it is probable that the data listed in Table I represent averages over a considerable region in each crystal. The dislocation densities were calculated from the strain broadening (N_ϵ) and from the tilt broadening (N_α) and these are also listed in Table I. Although some inconsistencies are evident, the agreement is reasonably good and it was concluded that the x-ray technique was capable of providing reliable average dislocation densities.

The rocking curves after straining were particularly inhomogeneous because of the discontinuous deformation and no attempt was made to calculate the dislocation densities from these data.

The inhomogeneities in half width along the crystals were probably due to large differences in substructure. One probable source of substructure boundaries appeared to be associated with the large number of dislocations left grain boundaries "ghosts" during the strain anneal crystal growing technique. Observations of "remembered grain boundaries" on deep etched specimens tend to confirm this idea. Many single crystals, as proved by x-ray Laue pictures, exhibited this phenomonon as shown in Figure 2, after deep etching. The grain size of the specimens, before strain-anneal crystal growing, is the same approximate size as the markings seen on the sample in Figure 2. Figure 3 shows a deformation twin in a single crystal that was pulled

in tension at -150°C. Note that the twin is bent, thus a discontinuity in orientation even though no grain boundary is present. In Figure 4 a grain boundary is shown with a twin running straight across the boundary. This appears to be a boundary left behind the advancing grain boundary during the crystal growth process. This might be caused by the very slight difference in orientation between this grain and that which was growing.

B. Etch-Pit Investigation

Samples of as grown crystals were etched in Frye's reagent after electropolishing. Dislocation densities were measured and are listed in Table II. A comparison with Table I shows that the etch pit densities correlate well with the dislocation densities calculated from the rocking curves. A few crystals were strained at room temperatures, heated at 15 min at 175°C to decorate the etch pit, and the dislocation densities were measured. This decoration technique has been used for silicon-iron and appeared to be sufficient to bring out all of the etch pits. The resultant data are shown in Table III. The dislocation densities increased by a factor of about 10^2 with strains of 0.4 to 2.3 percent.

Surface replicas were taken from several crystals and examined at 7,000 and 10,000X with an electron microscope. Typical electron micrographs are shown in Figures 5 and 6. The dislocation densities obtained by this method agreed with the optical microscopy counts within a factor of two. In Figure 5 it should be noted that the etch pits intersect the (100) surface on a (110) line.

C. Tensile Testing

Low temperature tensile tests were made on forty-six single and bicrystals of iron. Tests were

conducted over the temperature range from - 97°C to -196°C. The strain rate was maintained at .025 in/in/min.

Table IV lists the test temperature, carbon content, dislocation density and mechanical properties of each specimen. The column marked elongation lists only the elongation which occurred by a process of slip or cracking. In certain instances some extension by twinning took place in specimens which showed little or no slip, but in almost all specimens which exhibited extensive twinning, measurable amounts of slip took place.

The maximum stress resolved normal to the (001) is, in most cases, the resolved fracture stress based on the load at fracture. However no attempt was made to evaluate the fracture stress in specimens which necked prior to fracture because of the uncertainty in the determination of the true area at fracture. In these cases the tabulated value is the stress which the crystal was able to support without cleavage.

Many of the crystals had small parasite surface grains and in some cases these were involved with the fracture. In these cases we may infer that the true cleavage stress was higher than that reached during the tensile test. In many of the specimens tested at the higher temperatures, the extension of the specimen noted on the stress strain curve was a combination of slip and extension of the specimen by cracking of these parasite grain boundaries.

Figure 7 shows the elongation of the specimens as a function of carbon content and testing temperature. It is evident that carbon content plays a major role in the amount of slip observed in iron single crystals and there appears to be a range of carbon (about .002%) above which this ductility is uniformly low in the temperature

range used in these tests. Below .002% carbon, there is a trend toward a lower transition temperature, as the carbon content decreases.

Figure 8 illustrates the temperature dependence of the critical resolved shear stress, independent of carbon content, for crystals in which the first detectable plastic flow took place by slip. A similar relationship between temperature and yield by twinning is shown in Figure 9. In this connection yield was considered to have taken place by twinning only when a discontinuous drop in load (accompanied by an audible click) could be observed in the stress-strain curve. Metallographic examination of fractured specimens showed that the load-time curve was a suitable means of distinguishing between slip yield and twinning yield. It can be seen in Figures 8 and 9 that there was an apparent increase in the resolved yield stress in both cases but the increase in the yield stress for slip was much more marked.

Nearly all of the specimens which yielded by slip had carbon contents below .002% but even in these specimens, yield by twinning became more frequent as the temperature decreased. Crystals containing more than .002% carbon always yielded by twinning at temperatures below -120°C.

The fracture stress resolved normal to the cube plane is shown in Figure 10 for a group of specimens which did not display any tendency to neck and whose fractures were not associated with parasite grain boundaries. They appear to be insensitive to testing temperature but are sensitive to carbon content.

Since the crystals used in this investigation were sheet specimens the orientation of the face normals may have influenced the mechanical behavior. The dependence of resolved normal stress on face orientation is shown

in Figure 10. However, little information can be gained from this, because the orientations of the faces, in most instances, are similar to the tensile axis orientations. Thus, face normals close to (001) appear to lead to low stresses and low ductilities, in contrast to those near (112); but the tensile axis of these specimens are close to the (001) plane and the effects of face normal cannot be separated out.

Two specimens were prestrained 0.4% and 4.2% at room temperature and tested immediately at sub-zero temperatures. This prestraining in both cases, prevented twinning in the samples. Four other specimens were prestrained 0.4%, 0.8%, 1.4% and 2.3% respectively, heated for 15 minutes at 175°C to decorate the dislocations, and then aged at room temperature for six months. In these specimens twinning was not completely suppressed in all cases.

By plotting the apparent transition temperature versus carbon content, obtained from Figure 7, a line showing the dependence of transition temperature on carbon content is obtained. This line shown in Figure 11 is of the form:

$$C = A \exp. (BT)$$

where C is the carbon concentration, T is the transition temperature and A and B are constants.

D. Metallography of Fractured Specimens

The crystals, tested at temperatures lower than - 140°C, that exhibited large amounts of elongation also were found to have either grain boundary cracking around the small parasite grains or cracking in the twins and twin boundaries. The grain boundary cracking in some

cases isolated completely the parasite grains from the matrix. This is shown in Figure 12. The cracking of the twins was definitely proven in eight crystals and suspected in many others. Some of these samples are shown in Figure 13 through 16. The cracks in the twins appear to be steps whose wider sections are perpindicular to the gage length. One sample that exhibited these cracks was mounted and polished to determine the extent of the cracks in the sample. The cracks extend through the entire cross-section and a photomicrograph of this is shown in Figure 17. In Table V are shown the carbon contents, testing temperatures and orientations of the specimens that exhibited the twin cracking. These data show the tensile axis orientation was not a significant factor in the cracking or not cracking of twins.

Cracks in the matrix were found in some of the fractured specimens and examples of these are shown in Figures 18 and 19. In the specimens that exhibited cracking of the parasite grain boundaries, many cracks were found in the matrix that originated at a cracked grain boundary, but for some reason did not continue across the specimen to cause cleavage of the specimen.

IV. SUMMARY

The following points are evident from this series of tensile tests:

1. There is a large increase in transition temperature with increasing carbon content in the range from 0.0005 to 0.030 weight percent.

2. Very slight pre-straining, immediately before sub-zero testing, inhibits twin formation in iron single crystals.

3. Tensile axis orientation effects the mechanical properties considerably, with the specimens whose tensile axis is closest to the (001) plane, having a lower transition temperature.

4. Micro-cracks are formed in the twins when slip occurs after formation of the twins.

5. The formation of micro-cracks in the twins is not a function of tensile axis orientation.

6. Stable micro-cracks are formed that do not traverse the entire width of the crystal.

REFERENCES

1. N. Stroh, Adv. in Physics 6 (1957) 418.

2. A.H. Cottrell, Trans. Met. Soc. AIME 212 (1958) 192.

3. G.T. Hahn, B.L. Averbach, W.S. Owen and Morris Cohen Fracture, Wiley, 1959.

4. To be published.

5. M.J. Hordon and B.L. Averbach, Acta Met. 9 (March 1961) 247.

6. R.W. James, "The Optical Principles of the Diffraction of X-Rays", G. Bell and Sons, London, 1948.

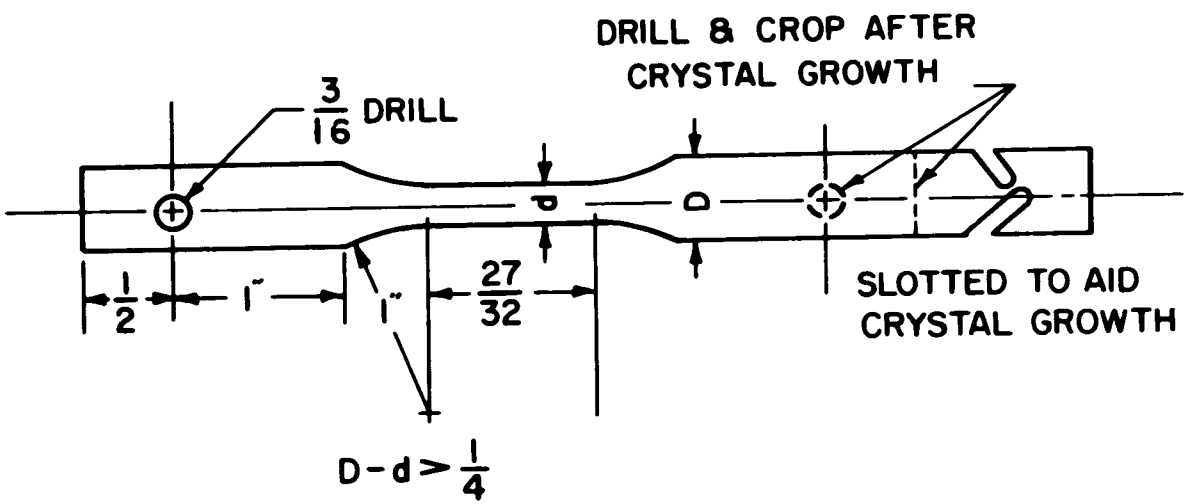

FIG. 1 TENSILE SPECIMEN

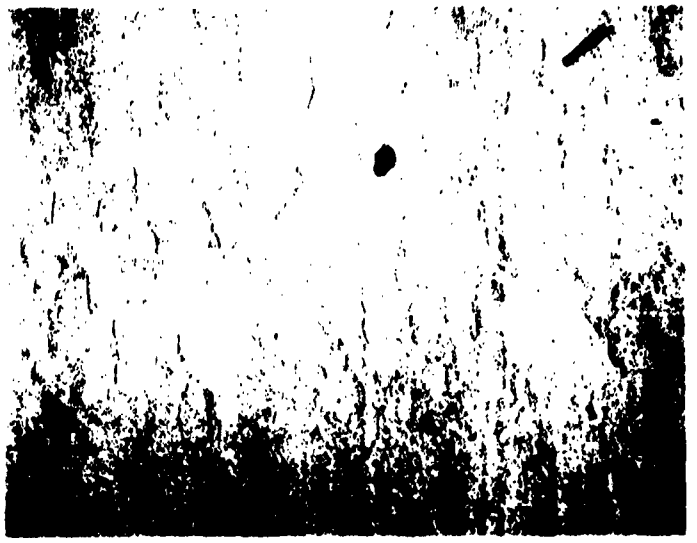

Figure 2 10X
"Remembered Grain Boundaries" in deep etched single crystal of iron.

Figure 3 1000X
Deformation twin in single crystal after testing in tension at 150°C. Note twin is bent indicating fairly large change in crystal orientation.

Figure 4 1000X

Deformation twin running
across grain boundary.

Figure 5 50,000X
Etch-pits on crystal having face orientation close to (100).
Electron micrograph from replica.

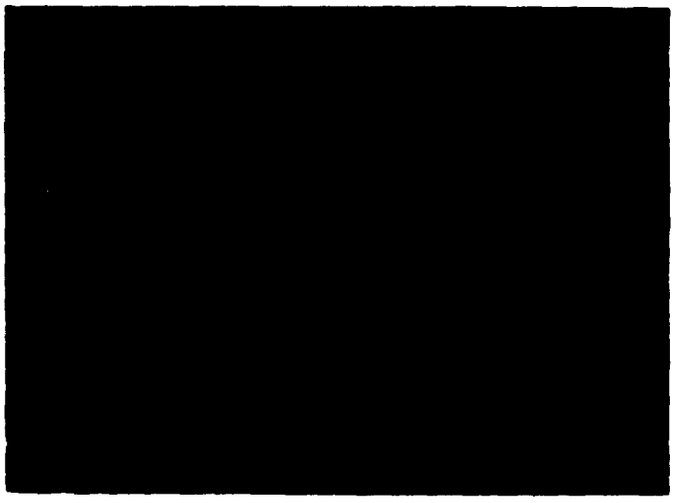

Figure 6 50,000X
Etch-pits on crystal having face orientation close to (112).
Electron micrograph from replica.

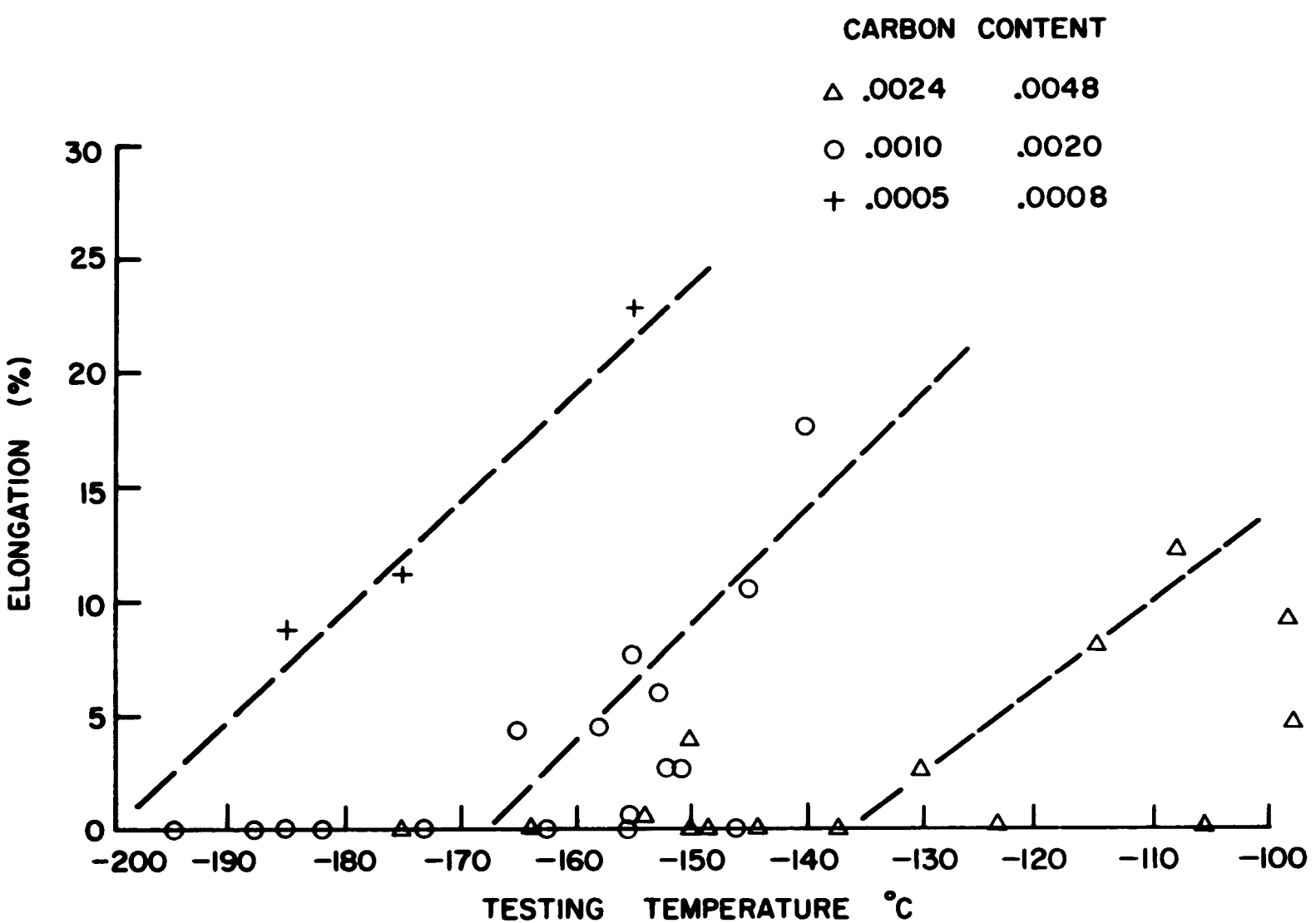

FIGURE 7. PERCENT ELONGATION vs. TESTING TEMPERATURE FOR IRON SINGLE CRYSTALS

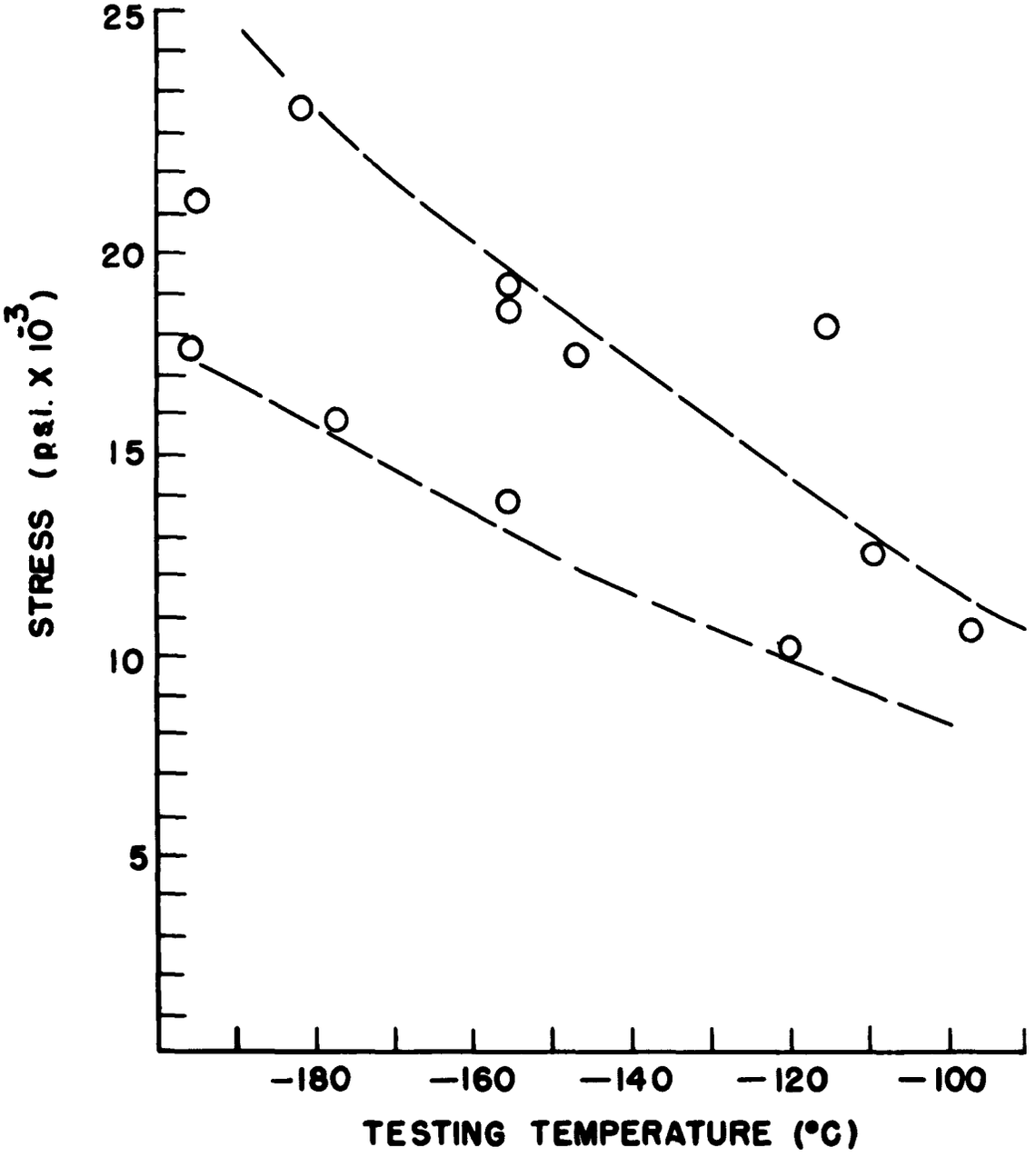

FIGURE 8. CRITICAL RESOLVED SHEAR STRESS FOR SLIP AS A FUNCTION OF TESTING TEMPERATURE

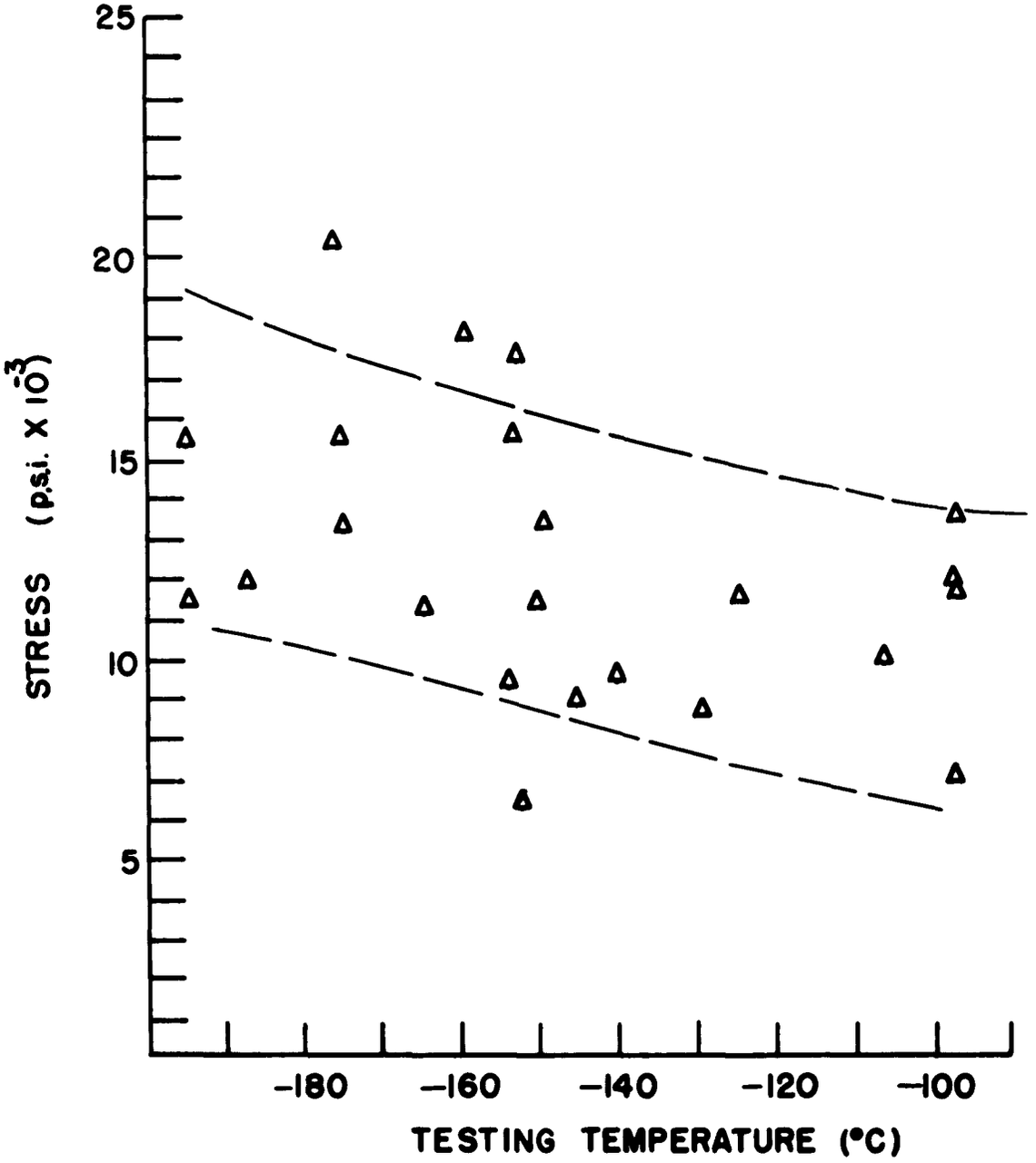

FIGURE 9. CRITICAL RESOLVED SHEAR STRESS FOR TWINNING AS A FUNCTION OF TESTING TEMPERATURE

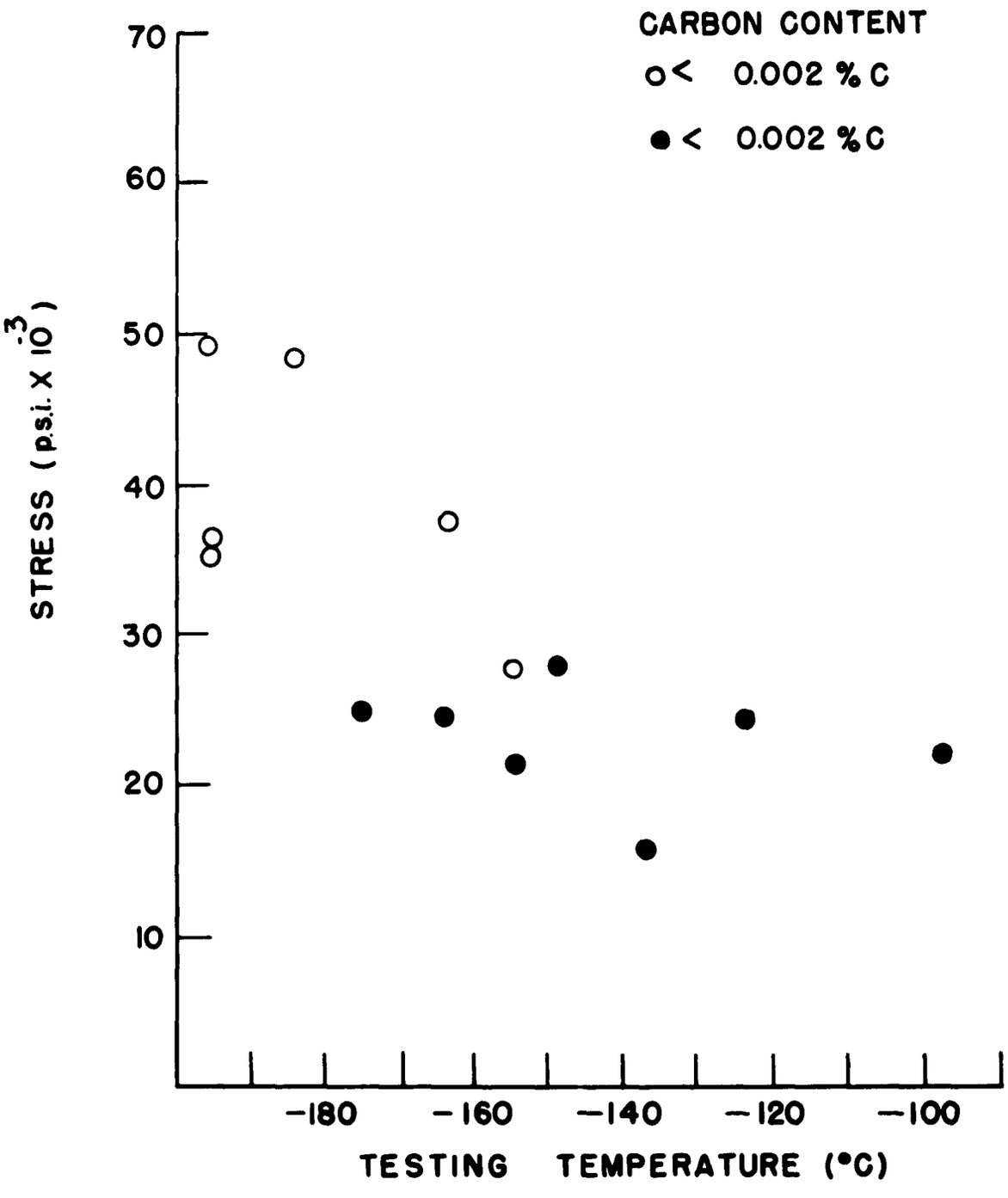

FIGURE 10. FRACTURE STRESS RESOLVED NORMAL TO CUBE PLANE

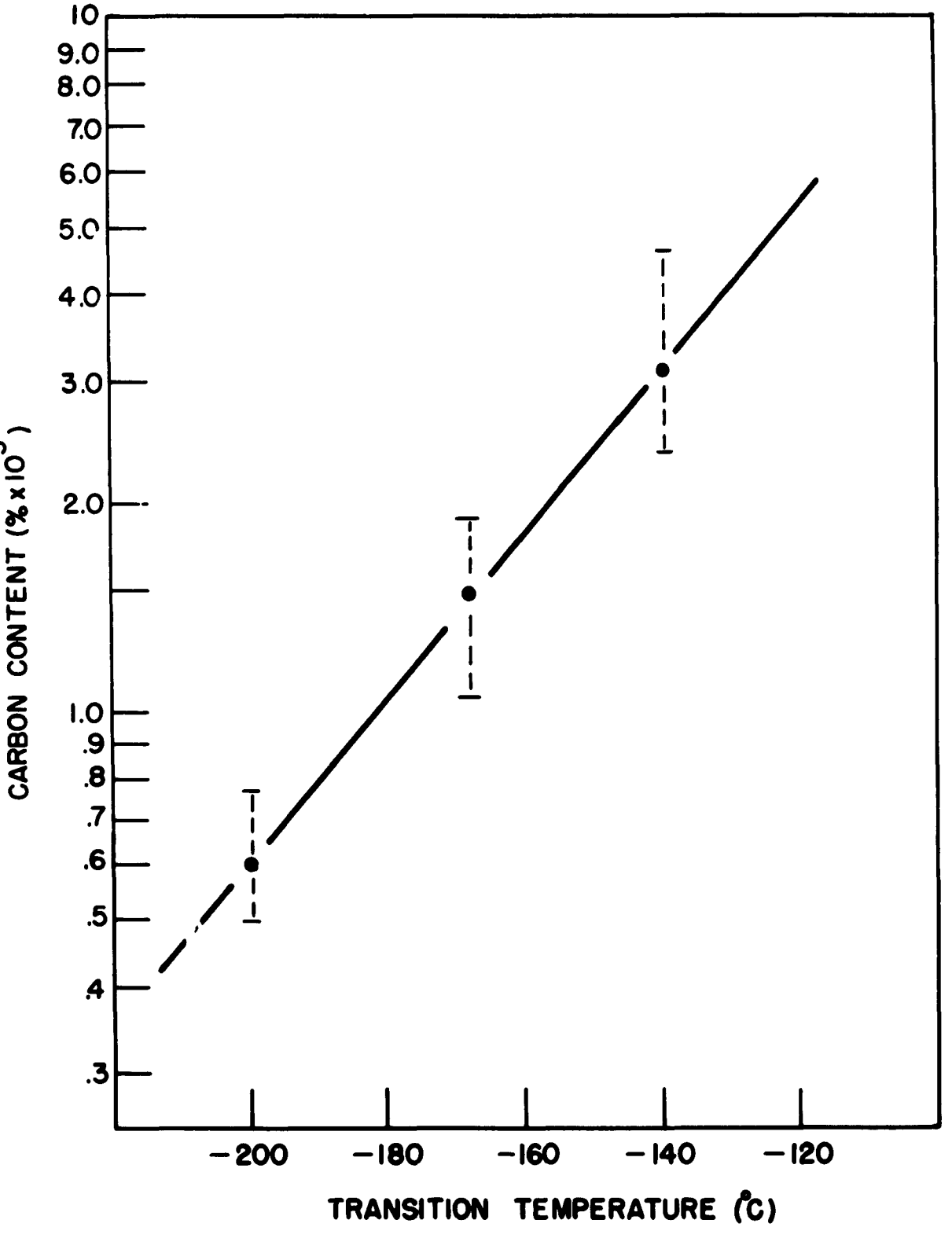

FIGURE II TRANSITION TEMPERATURE vs. CARBON CONTENT

Figure 12 1000X
Cracking of parasite grain boundaries with associated micro-cracks in Matrix.

Figure 13 1000X
Micro-cracks in twins in iron single crystal.

Figure 14 1000X
Micro-cracks in twins in iron single crystal.

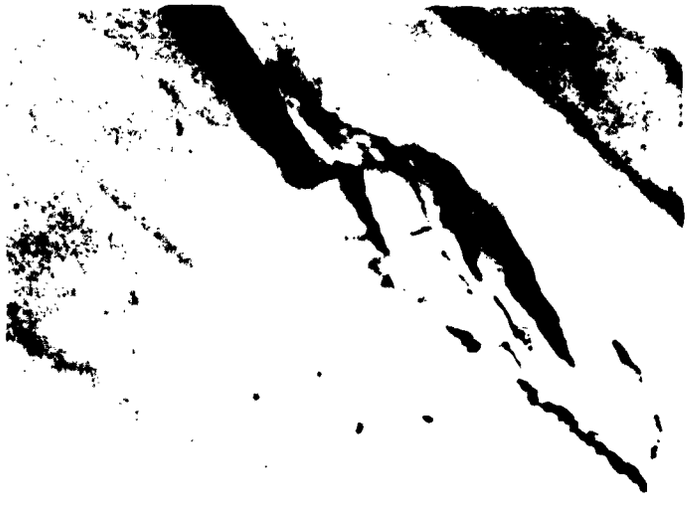

Figure 15 1000X
Micro-crack formed at twin intersection in iron single crystal.

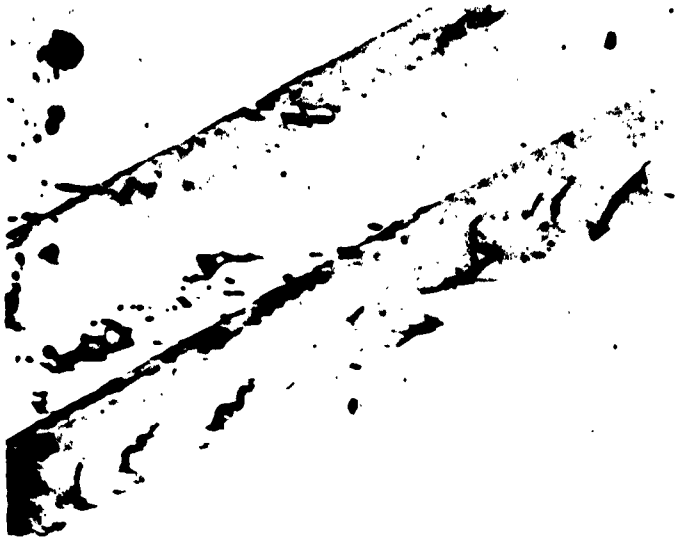

Figure 16 1000X
Micro-cracks in twins in iron single crystal.

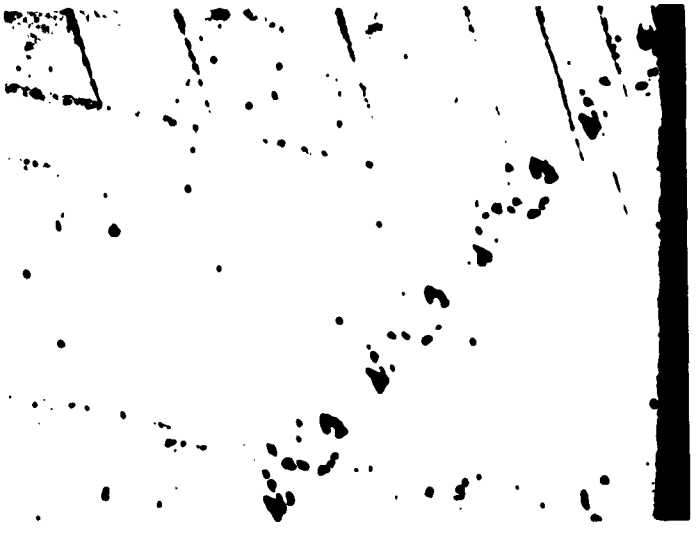

Figure 17 200X
Transverse section of single crystal with micro-cracks in twins. Note cracks and voids still visible in twins.

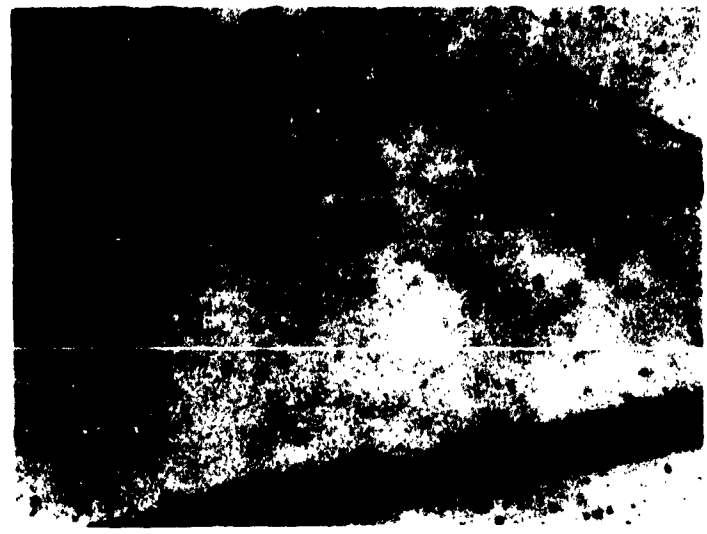

Figure 18 1000X
Micro-crack in Matrix of iron single crystal.

Figure 19 1000X
Micro-crack in matrix associated with intersection of twin and cracked grain boundary.

TABLE I

Half-Breadths of (200) Diffraction Peaks for Various X-Ray Wavelengths and the Dislocation Densities Calculated from Them

Sample	$\beta_m(CuK_\alpha)$	$\beta_m(CrK_\alpha)$	$N_\alpha(10^7 Cm^{-2})$	$N_\epsilon(10^7 Cm^{-2})$
4S-11	2.78	1.96	8	9
4S-13	4.45	2.45	6	32
4S-15	2.75	1.30	0.2	14
4S-25	1.83	1.51	6	3
4S-40	2.15	1.63	7	5
4S-49	3.47	1.59	5	22
4S-50	2.17	1.11	0.6	8
6S-7	2.50	1.55	4	9
R-5	2.33	1.44	3	8
R-8	2.71	1.92	8	8
R-9	3.03	1.89	6	13
T-1	1.72	1.24	7	1

Half-Breadths of (200) Diffraction Peaks Measured Before and After Straining

Sample	Condition	$\beta_m(CuK_\alpha)$	$\beta_m(CrK_\alpha)$
4S-50	As Grown	2.17	1.11
	after 0.4% strain	3.07	3.35
6S-7	As Grown	2.50	1.55
	after 0.8% strain	2.89	2.82
4S-15	As Grown	2.75	1.30
	after 2.3% strain	11.6	10.1

TABLE II

Dislocation Densities as Measured by Etch Pit Techniques

Sample	Dislocation Density ($10^7 Cm^{-2}$)	Sample	Dislocation Density ($10^7 Cm^{-2}$)
4S-11	8	15	-
4S-13	5	16	-
4S-15	8	17	6
4S-25	6	18	-
4S-30	5	23	5
4S-33	8	57	3
4S-39	4	95	3
4S-49	5	96	5
4S-50	6	105	3
6S-7	6	115	2
R-5	6	120	4
R-8	6	126	3
R-9	8	128	3
T-1	4	131	4
T-2	3	135	6
T-3	3	145	5
T-5	2	152	4
X	3	153	4
4	-	159	3
11	6	170	4
12	6	185	4
14	8		

TABLE III

Dislocation Densities Measured Before and After Straining Various Amounts By Etch Pit Techniques

Sample	% Strain	Dislocation Density	
		Before Straining	After Straining
4S-15	2.3	8×10^7	14×10^9
4S-33	1.4	6×10^7	7×10^9
6S-7	0.8	6×10^7	3×10^9
4S-50	0.4	6×10^7	6×10^9
4S-39	0.4	4×10^7	6×10^9

TABLE IV

Tensile Data and Other Pertinent Facts
for Fractured Iron Single Crystals

Test Temperature (°C)	Sample	Tensile Axis Orientation	Carbon Content (%)	Dislocation Density ($10^7 cm^{-2}$)	Elongation (%)	Resolved Critical Shear Stress psix(10^{-3}) Slip	Resolved Critical Shear Stress psix(10^{-3}) Twinning	Maximum Normal Stress (psix10^3)
-196	6S-7	(100)	.0010	6	0		11.5	23.8**
-196	4S-39	(112)	.0010	4	0	17.7		36.2
-196	4S-49	(321)	.0010	5	0	21.2		35.6
-196	4S-50	(110)	.0013	6	0		15.5	48.6
-188	15	(100)	.0018	-	0		14.6	41.0**
-187	4S-15	(110)	.0005	8	7		12	48.1
-182	4S-33	(110)	.0011	6	0	23.5		37.7**
-177	R-9	(112)	.0007	8	12	15.6		54.5*
-175	37	(100)	.0036	3	0		15.6	24.9
-175	128	(110)	.0019	3	5.3		14.3	48.2*
-173	11	(100)	.0015	6	0			51.2
-164	170	(100)	.0034	4	0		11.3	24.4
-163	18	(100)	.0019		0	18.8		37.8
-158	4S-11	(110)	.0023	8	4		18.2	39.4**
-155	T-1	(100)	.0015	4	0.2	13.7		27.7
-155	95	(100)	.0022	3	0			36.8
-155	131	(100)	.0034	4	0			38.8
-155	R-5	(112)	.0008	6	8	19		38.2*
-155	R-8	(100)	.0005	6	23.0	18.7		65.5*

* Not a fracture stress
** Fracture occurred in or initiated in parasite grain boundary

TABLE V

Tensile Axis Orientation and Other Data for Single Crystals that Exhibited Cracking in Twins

Sample	Carbon(%)	Dislocation Density ($10^7 Cm^{-2}$)	Testing Temperature (°C)	Tensile Axis Oreientation
16	.0020	-	-140	(112)
12	.0020	6	-145	(100)
126	.0016	3	-152	(112)
4	.0017	-	-152	(111)
4S-11	.0023	8	-158	(110)
128	.0019	3	-175	(210)
R-9	.0007	8	-177	(112)
4S-15	.0005	8	-187	(110)

ALLOYD ELECTRONICS CORPORATION, Cambridge, Mass., INFLUENCE OF CARBON CONTENT AND SUBSTRUCTURE ON CLEAVAGE IN IRON SINGLE CRYSTALS, by D.A. Hay and B.L. Averbach, April 1962

33p. incl. illus. tables, 6 refs. (Project 7021)(Contracts AF 33(616)-6454 and AF 33(616)-7091, Phase I) (ASD TR 61-686)

Unclassified Report

The influence of substructure and carbon content on the ductile-brittle transition temperature were studied in iron single crystals. It was found that increases in carbon content (from 0.005% to 0.030% raised the transition temperature considerably. Small amounts of pre-straining at room temperature before sub-zero testing inhibited twin formation. In cases where twins were formed, many micro-cracks were found in twins and at twin boundaries in fractured crystals. In some cases, micro-cracks were also found in the matrix of fractured crystals.

UNCLASSIFIED

ALLOYD ELECTRONICS CORPORATION, Cambridge, Mass., INFLUENCE OF CARBON CONTENT AND SUBSTRUCTURE ON CLEAVAGE IN IRON SINGLE CRYSTALS, by D.A. Hay and B.L. Averbach, April 1962

33p. incl. illus. tables, 6 refs. (Project 7021)(Contracts AF 33(616)-6454 and AF 33(616)-7091, Phase I) (ASD TR 61-686)

Unclassified Report

The influence of substructure and carbon content on the ductile-brittle transition temperature were studied in iron single crystals. It was found that increases in carbon content (from 0.005% to 0.030% raised the transition temperature considerably. Small amounts of pre-straining at room temperature before sub-zero testing inhibited twin formation. In cases where twins were formed, many micro-cracks were found in twins and at twin boundaries in fractured crystals. In some cases, micro-cracks were also found in the matrix of fractured crystals.

UNCLASSIFIED